Supporting Information for "Tundra photosynthesis captured by satellite observed solar-induced chlorophyll fluorescence"

K. A. Luus[1], R. Commane[2], N. C. Parazoo[3], J. S. Benmergui[2],

S. E. Euskirchen[4], C. Frankenberg[5], J. Joiner[6], J. Lindaas[2,7], C. E. Miller[3],

W. C. Oechel[8,9], D. Zona[8,10], S. Wofsy[2], and J. C. Lin[11]

Corresponding author: K.A. Luus, (kaluus@uwaterloo.ca)

[1]Centre for Applied Data Analytics Research, Dublin, Ireland

[2]Harvard School of Engineering and Applied Sciences, Cambridge MA 02138, USA

[3]NASA Jet Propulsion Lab, 4800 Oak Grove Drive, Pasadena, CA 91109, USA

[4]Institute of Arctic Biology, University of Alaska Fairbanks, 902 N. Koyukuk Dr. P.O. Box 757000, Fairbanks, AK 99775, USA

[5]Environmental Science & Engineering, California Institute of Technology, CA 91125, USA

[6]NASA Goddard Space Flight Center, Greenbelt, MD 20771, USA

[7]Department of Atmospheric Science, Colorado State University, Fort Collins, CO, 80523

Key Points.

Abstract.

[8]San Diego State University, San Diego, CA 92182, USA

[9]The Open University, Walton Hall, Milton Keynes MK7 6AA, UK

[10]University of Sheffield, Sheffield, South Yorkshire S10 2TN, UK

[11]University of Utah, Salt Lake City, UT 84112, USA

Contents

S1 - Introduction

The improved capacity of SIF to capture tundra photosynthesis, relative to EVI, has important implications for accurately estimating Alaska's carbon cycling. The findings presented in this section examine agreement between site-scale eddy covariance NEE and modeled NEE at four Alaskan sites, and discrepancies between mean annual EVI and SIF across Alaska as they relate to vegetation types. These results confirm that biases arise mainly from tundra regions within Alaska. An examination is then provided of CARVE-optimized NEE relative to PolarVPRM-EVI and PolarVPRM-SIF, which indicates that using SIF instead of EVI substantially improves accuracy in modeling Alaska's carbon balance. A final comparison of time series of EVI-based and SIF-based Alaskan GPP, relative to MODIS GPP, further highlights that biases arising from reliance on vegetation indices may be widespread.

S2 - Results: Alaskan Site-Scale NEE

The spring bias in EVI-based NEE arises mainly from sedge, bog and tussock tundra sites [Figure S1 g–l]. These regions play an important role in Arctic carbon cycling, causing regional biases in model estimates. The differences in PolarVPRM-SIF and PolarVPRM-EVI are much smaller across barren and wetland regions. [Figure S1c & f].

S3- Results: Alaskan EVI and SIF

Across Alaska, mean EVI and SIF values follow a similar seasonal course over time and between years: EVI remains elevated (>0) throughout most of the snow season, and both increases earlier in spring than SIF and declines later in fall than SIF [Figure S2]. MODIS EVI displays greater inter-annual variability than GOME-2 SIF.

Relative to SIF, EVI displays larger variability in peak annual values across shrub and graminoid tundra regions [Figure S3]. Specifically, large (>0.55) maximum annual values of EVI are observed within graminoid tundra regions north of the Brooks Range, and in shrub tundra areas south of Denali Mountains [Figure S4]. These values exceed maximum annual EVI values detected across forested areas, indicating errors potentially arising from topographic effects.

When the tendency for site-scale photosynthesis to be overestimated by PolarVPRM-EVI at tundra sites [Figure S1 g–l] is considered in context of the aforementioned indications that EVI is large (>0.55) expected and remains elevated (>0) for a longer time than expected across tundra regions, it becomes clear that photosynthesis is overestimated by EVI-based approaches across tundra regions.

S4 - Results: Alaskan Regional NEE

The implications of biases in EVI-based tundra photosynthesis relative to SIF-based photosynthesis for estimates of Alaska's carbon cycle are shown here, through comparisons of modeled and CARVE-optimized NEE. In Figure S5, the mean monthly additive flux required to bring PolarVPRM-EVI and PolarVPRM-SIF in line with CARVE-optimized NEE is indicated, as well as the influence of these differences for the mean annual seasonal cycle of NEE.

Examinations of spatially averaged estimates of GPP (-GEE) from EVI-based & SIF-based PolarVPRM, and MOD17A2 GPP, indicated similar seasonal patterns of photosynthesis from both MODIS-based approaches [Figure S6]. When GPP was estimated using SIF rather than EVI, growing season length and springtime GPP were reduced, resulting in diminished estimates of total annual GPP across Alaska.

References

Jung, M., K. Henkel, M. Herold, and G. Churkina (2006), Exploiting synergies of global land cover products for carbon cycle modeling, *Remote Sensing of Environment*, *101*(4), 534–553.

Luus, K., Y. Gel, J. Lin, R. Kelly, and C. Duguay (2013), Pan-Arctic linkages between snow accumulation and growing-season air temperature, soil moisture and vegetation, *Biogeosciences*, *10*, 7575–7597.

Running, S. W., and M. Zhao (2015), Daily GPP and Annual NPP (MOD17A2/A3) products NASA Earth Observing System MODIS land algorithm.

Walker, D. A., M. K. Raynolds, F. J. Daniëls, E. Einarsson, A. Elvebakk, W. A. Gould, A. E. Katenin, S. S. Kholod, C. J. Markon, E. S. Melnikov, et al. (2005), The circumpolar arctic vegetation map, *Journal of Vegetation Science*, *16*(3), 267–282.

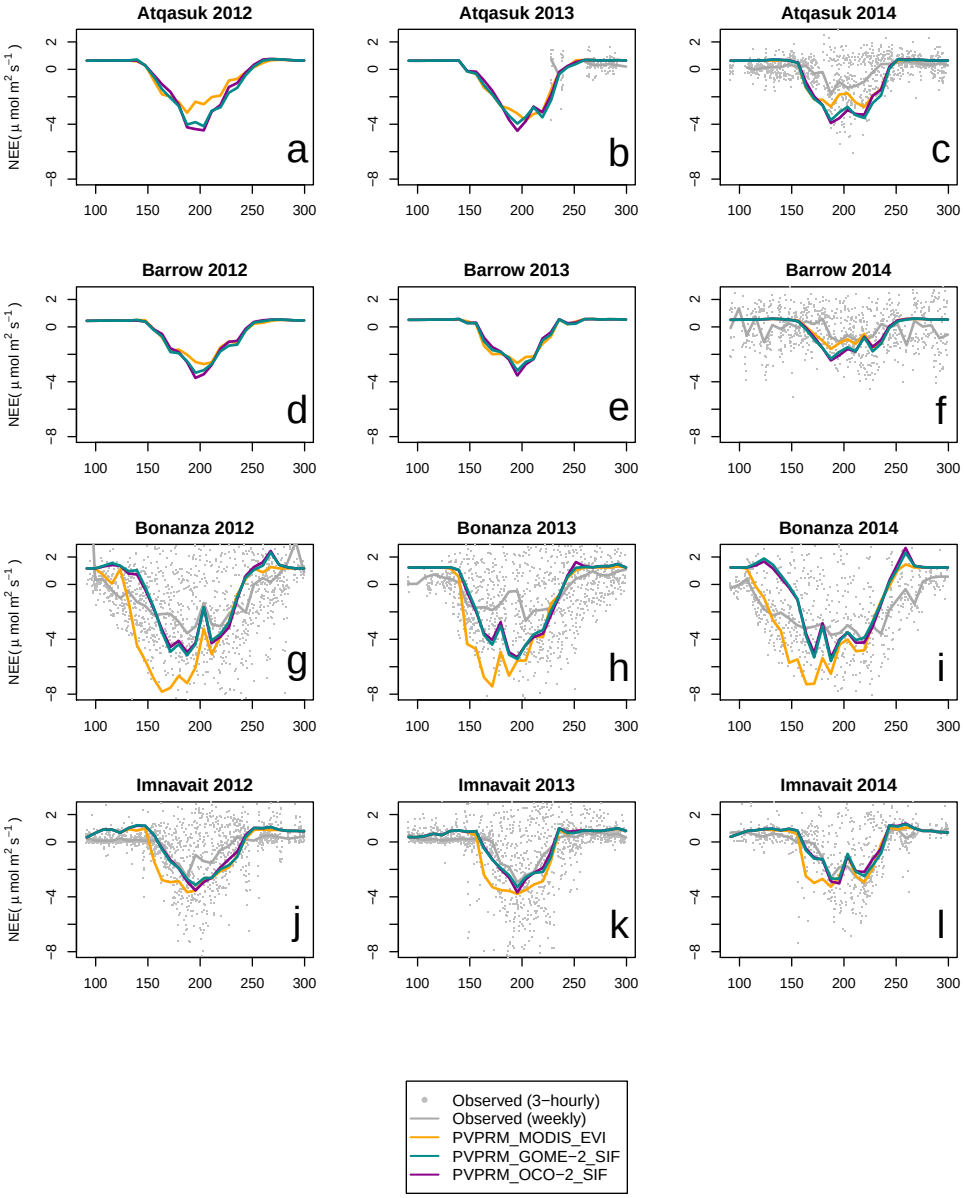

Figure S1. PolarVPRM NEE estimated from MODIS EVI and GOME-2 SIF at four Alaskan eddy covariance sites: Atqasuk (a–c), Barrow (d–f), Bonanza (g–i) and Imnavait (j–l), in 2012 (left column), 2013 (middle column) and 2014 (right column).

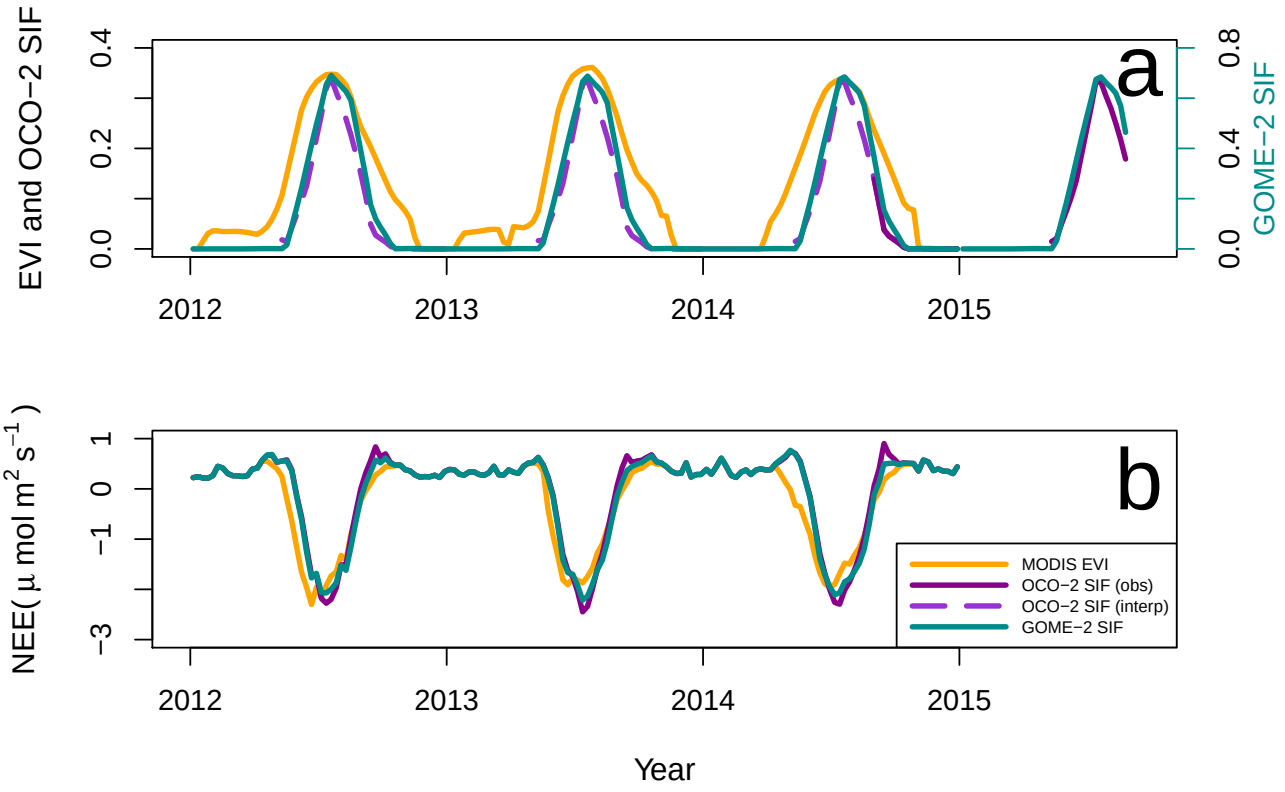

Figure S2. Time series (2012–2014) of spatially averaged Alaskan a) MODIS EVI, GOME-2 SIF/cos(SZA) and OCO-2 SIF/cos(SZA); and b) modelled NEE ($\frac{\mu\text{mol}}{\text{m}^2\text{s}}$): PolarVPRM-EVI, and PolarVPRM-SIF (from GOME-2 SIF, and OCO-2 SIF).

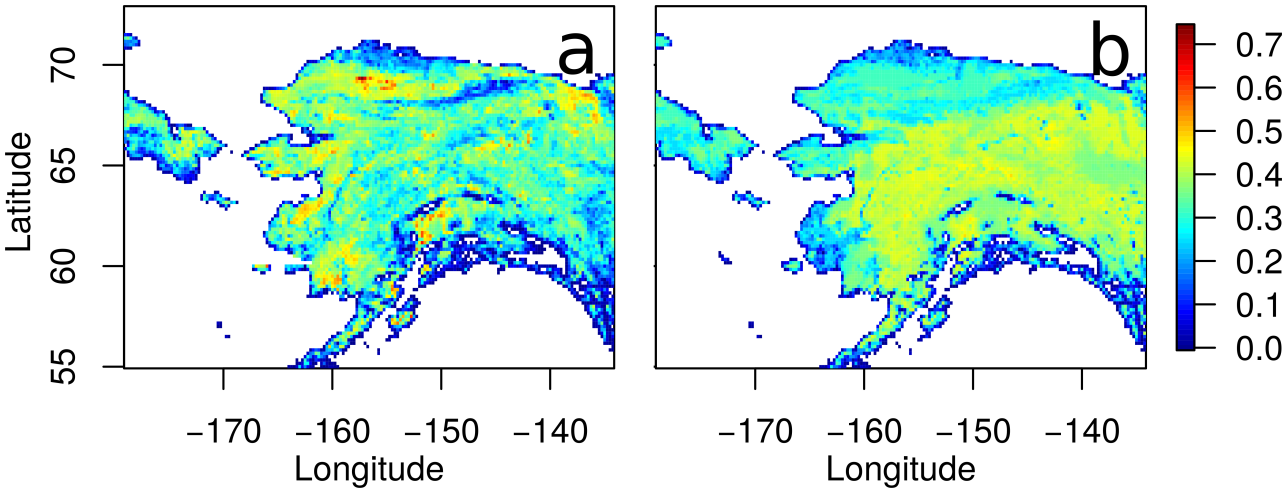

Figure S3. Maximum annual MODIS EVI (2014) (a) and maximum annual OCO-2 SIF (b) across Alaska.

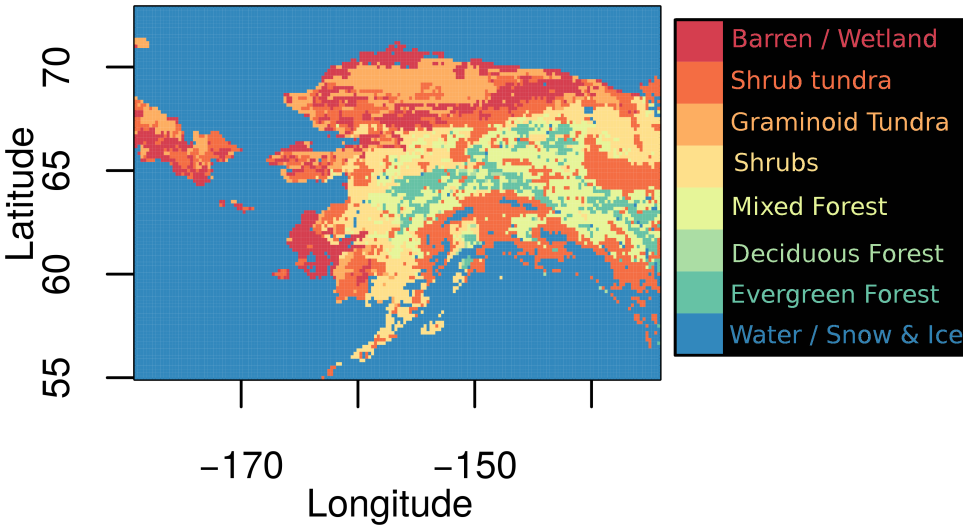

Figure S4. Predominant cover by fractional vegetation class, used in generating PolarVPRM estimates of NEE.Fractional vegetation classes were acquired by combining the Circumpolar Arctic Vegetation Map (CAVM) [*Walker et al.*, 2005] and Synergistic Land Cover Map (SYNMAP) [*Jung et al.*, 2006], as described in [*Luus et al.*, 2013].

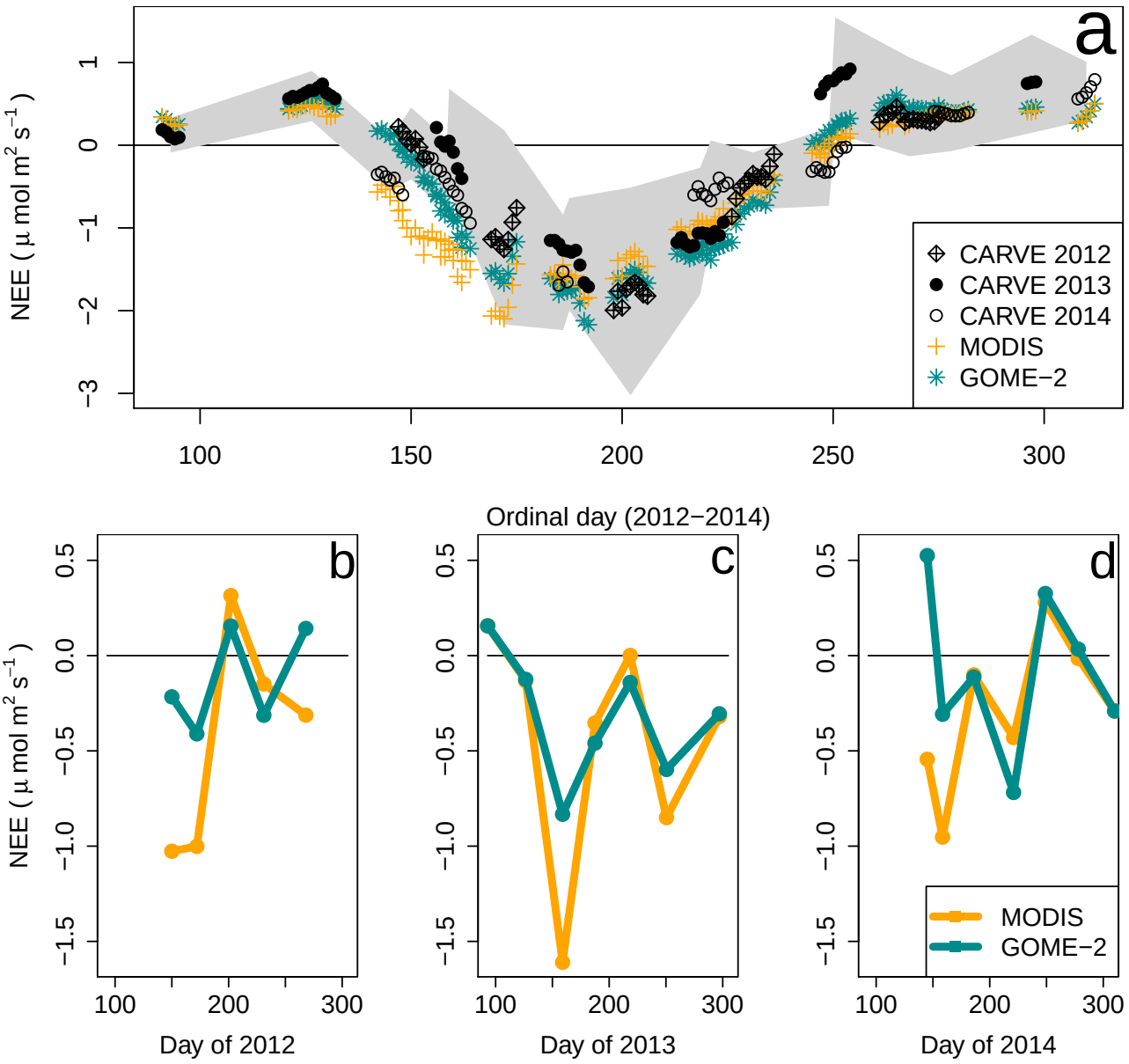

Figure S5. Spatially averaged Alaskan NEE from CARVE, and simulated using MODIS EVI and GOME-2 SIF (2012–2014). The seasonal cycle of CO_2 for all three years is indicated in a), where the shaded area indicates the standard deviation of monthly CARVE-adjusted NEE, overlaid for all three years. The monthly average δF flux correction values required to bring CARVE column profiles in line with PolarVPRM-SIF NEE (turquoise) or PolarVPRM-EVI NEE (orange) are indicated separately for b) 2012, and c) 2013 and d) 2014.

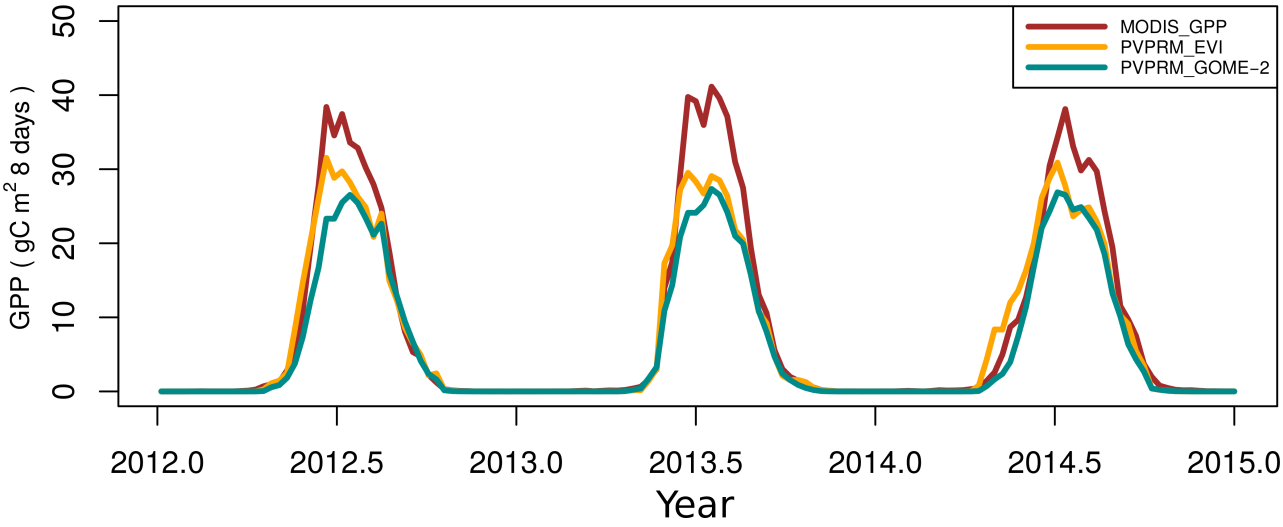

Figure S6. Mean Alaskan spatially-averaged estimates of GPP from the MODIS MOD17A2 GPP product, and from PolarVPRM estimates of GEE using MODIS EVI and GOME-2 SIF (in $\frac{\text{gC}}{\text{m}^2}$ per eight days). MOD17A2 calculates GPP using an NDVI-driven approach similar to PolarVPRM EVI: $GPP = \epsilon \cdot T_{\text{scale}} \cdot W_{\text{scale}} \cdot \text{APAR}$, where ϵ_{max} is equivalent to λ in PolarVPRM, and APAR is calculated as fPAR·PAR, where fPAR≈NDVI [*Running and Zhao*, 2015].